The Cryosphere Discuss., 5, 1055–1088, 2011
www.the-cryosphere-discuss.net/5/1055/2011/
doi:10.5194/tcd-5-1055-2011

The Cryosphere Discussions

Modelling the 20th and 21st century evolution of Hoffellsjökull glacier, SE-Vatnajökull, Iceland

G. Aðalgeirsdóttir[1,2], S. Guðmundsson[1], H. Björnsson[1], F. Pálsson [1], T. Jóhannesson[3], H. Hannesdóttir[1], S. Þ. Sigurðsson[4], and E. Berthier[5]

[1]Institute of Earth Sciences, University of Iceland, 101 Reykjavík, Iceland
[2]Danish Meteorological Institute, 2100 Copenhagen, Denmark
[3]Icelandic Meteorological Office, Bústadavegi 150, 105 Reykjavík, Iceland
[4]Department of Computer Science, University of Iceland, 107 Reykjavík, Iceland
[5]CNRS; Université de Toulouse, Laboratoire d'Etudes en Géophysique et Océanographie Spatiales (LEGOS); 14 Av. Ed. Belin, 31400 Toulouse, France

Received: 21 March 2011 – Accepted: 24 March 2011 – Published: 6 April 2011

Correspondence to: G. Aðalgeirsdóttir (gua@dmi.dk)

Published by Copernicus Publications on behalf of the European Geosciences Union.

Modelling the 20th and 21st century evolution of Hoffellsjökull glacier

G. Aðalgeirsdóttir et al.

Abstract

The Little Ice Age maximum extent of glaciers in Iceland was reached about 1890 AD and most glaciers in the country have retreated during the 20th century. A model for the surface mass balance and the flow of glaciers is used to reconstruct the 20th century retreat history of Hoffellsjökull, a south-flowing outlet glacier of Vatnajökull, which is located close to the southeast coast of Iceland. The bedrock topography was surveyed with radio-echo soundings in 2001. A wealth of data are available to force and constrain the model, e.g. surface elevation maps from ~1890, 1936, 1946, 1986, 2001, 2008 and 2010, mass balance observations conducted in 1936–1938 and after 2001, energy balance measurements after 2001, and glacier surface velocity derived by DGPS and correlation of SPOT5 images. The 21% volume loss of this glacier in the period 1895–2010 is realistically simulated with the model. After calibration of the model with past observations, it is used to simulate the future response of the glacier during the 21st century. The mass balance model was forced with an ensemble of temperature and precipitation scenarios from a study of the effect of climate change on energy production in the Nordic countries (the CES project). If the average climate of 2000–2009 is maintained into the future, the volume of the glacier is projected to be reduced by 30% with respect to the present at the end of this century, and the glacier will almost disappear if the climate warms as suggested by most of the climate change scenarios. Runoff from the glacier is predicted to increase for the next 30–40 years and decrease after that as a consequence of the diminishing ice-covered area.

1 Introduction

Iceland (103 000 km^2) lies in the North Atlantic Ocean, just south of the Arctic Circle. Due to the warm Irminger Current, the island enjoys a relatively mild and wet oceanic climate and a small seasonal variation in temperature. The average winter temperatures are around 0°C near the southern coast, where the average temperature of the warmest month is only 11°C and the mean annual temperature is about 5°C (Einarsson, 1984). At present about 11% of the country is covered by glaciers (Björnsson, 1978). The Icelandic ice caps are temperate, characterized by high annual mass turnover (1.5–3.0 m water equivalent (w.e.)) and are highly dynamic. They are sensitive to climate variations and have responded rapidly to changes in temperature and precipitation during historical times (Björnsson, 1979; Björnsson et al., 2003; Björnsson and Pálsson, 2008; Guðmundsson et al., 2011). The recorded volume and area changes of these glaciers are therefore good indicators of climate change.

Historical records of the glacier extent reach back to the settlement of Iceland in the late 9th century. During the settlement, glaciers were smaller than at present. They started to advance in the 13th century at the onset of the Little Ice Age that lasted until late 19th century when most glaciers in Iceland reached their maximum extent. In the 20th century, the climate was significantly warmer than during the Little Ice Age, with higher temperatures in the period 1930–1945 and again at the end of the century. Glaciers in Iceland have retreated during most of the 20th century with the exception of a standstill or an advance in 1960–1990 (Sigurðsson and Jóhannesson, 1998; Björnsson and Pálsson, 2008).

In this study, a Shallow Ice Approximation (SIA) ice-flow model coupled with a positive degree-day (PDD) mass-balance model (Aðalgeirsdóttir et al., 2006) is used to simulate the evolution of Hoffellsjökull outlet glacier of the Vatnajökull ice cap since its Little Ice Age maximum extent, and to predict the future response to an ensemble of climate change scenarios. Temperature and precipitation measurements from the meteorological stations Hólar in Hornafjörður (HH) and Fagurhólsmỳri (F), respectively, near the glacier (Fig. 1a), are used to force the coupled model. A sensitivity study of various model parameters and model assumptions is carried out and the ensemble of climate change scenarios (Jóhannesson et al., 2011) is used to assess the relative importance of natural climate variability on the one hand and a deterministic anthropogenic warming trend on the other for the evolution of the glacier during this century.

TCD
5, 1055–1088, 2011

2 Study area

Hoffellsjökull is a south-flowing outlet glacier of Vatnajökull, the largest ice cap in Iceland (Fig. 1). The accumulation zone is a part of the eastern sector of the ice cap between two mountains, Breiðabunga and Goðahnúkar, at 1350–1450 m elevation. From the accumulation area, the ice flows in two branches, west and east of the central nunatak Nỳju Núpar. The branches meet below the nunatak and the ice is funnelled through a 2 km wide ice fall at 600–700 m elevation where the elevation drops 300 m over a 4 km distance. Below the ice fall, the glacier spreads out on the lowland and terminates in a lagoon at ∼40 m a.s.l.

The first glaciological expeditions to this area were conducted in 1936–1938, when a group of Swedish and Icelandic glaciologists measured the ice flow, the surface mass balance and the surface topography. They also carried out a detailed analysis to understand the relative roles of accumulation and melting in the total mass balance of the glacier and to establish a relationship between the climate and the advance and retreat of the glaciers. Up to 8 m thick winter snow layer was measured in the accumulation area (∼4 m w.e). Ice melt of up 10 m w.e. was measured in the lowest part of the ablation zone in summer, in addition to 2 m w.e. that was melted during winter. Taking into account ∼2 m of annual rainfall, the runoff from this part of the glacier was estimated as ∼14 m w.e. per year; a surprisingly high value (Ahlmann, 1939, Ahlmann and Thorarinsson, 1943; Thorarinsson, 1939, 1943).

The glacier was revisited in 2001 when the surface and bed topography was mapped. Automatic weather stations were placed at 2 locations on and near the glacier and a still ongoing surface mass balance survey was initiated. In addition, the glacier mass balance has been measured since 1996 at four locations close to the ice divide of Hoffellsjökull to the west and north (Fig. 1c).

3 Observations

3.1 Geometry

Hoffellsjökull was surveyed with a radio-echo sounder and Differential Global Positioning System (DGPS) equipment in 2001. Continuous profiles, approximately 1 km apart, were measured in the accumulation zone and a dense network of point measurements were carried out in the ablation zone. Digital Elevation Models (DEMs) of the surface and bedrock were created from these data (Fig. 2; Björnsson and Pálsson, 2004). The estimated errors are at most 1–5 m (bias less than 1 m) for the surface map and depending on the location, 5–20 m for the bedrock map. Glacier extent and maps of the ice surface of Hoffellsjökull are available from the years 1904 (lowest parts, geodetic survey in summer), 1936 (geodetic survey in summer), 1946 (aerial photographs in autumn), 1988 (aerial photographs in autumn), 2001 (DEM from DGPS survey in spring), 2008 (DEM from SPOT5 HRS images in autumn, Korona et al., 2009) and 2010 (airborne Lidar in autumn).

The most accurate glacier map is the Lidar-DEM (5×5 m pixel resolution, with an accuracy of <20 cm in elevation and <0.5 m in position). It is used as a reference map for co-registering the SPOT5 HRS-DEM (pixel resolution of 40×40 m), using the ice free areas surrounding Hoffelssjökull and the correlation method described by Guðmundsson et al., (2011). This comparison revealed a horizontal shift of the HRS-DEM by 15 m and 5 m towards east and north, respectively, and a vertical offset of 2.3 m. These errors are within the nominal 15 m RMS accuracy in position and 5 m in elevation given for a raw HRS-DEM by Bouillon et al. (2006). Gaps in the HRS DEM, due to low contrast of the SPOT5 stereo image pairs at some sections in the accumulation area of Hoffellsjökull, were filled by smoothly adjusting the Lidar DEM to the HRS DEM. Available elevation values within the accumulation area were used to calculate the offset and tilting between the 2008 and 2010 DEMs. After correcting the HRS DEM with the Lidar DEM, we estimate the residual vertical bias error of the HRS DEM to be <0.5 m; as obtained in a similar study by Guðmundsson et al. (2011).

TCD
5, 1055–1088, 2011

The DEMs from before 2001 were created from digitized contour lines of the older maps (Fig. 2). The ice surface elevation of 1890 (Fig. 2b, Little Ice Age maximum, LIA_{max}) was reconstructed from the more recent surface DEMs assuming that although the surface has lowered significantly, the surface shape only changes slightly in the accumulation zone. The location of the LIA_{max} terminal moraines and the location and elevation of the side moraines on both sides of the glacier (Jónsson, 2004) as measured by DGPS were used in the reconstruction of the 1890 ice surface elevation of the lower part of the glacier as well as the ice surface map from 1904 which was used as a constraint for the shape. A conservative vertical error estimate for the reconstructed 1890 DEM is 15–20 m, 10–15 m for the 1936 DEM, 5–10 m for the 1946 DEM and 5 m for the 1986 DEM.

Additional information on glacier extent and glacier variations may be extracted from written historical descriptions of local farmers. They describe the land use (i.e. grassing of cattle and sheep, use of the forest growing in the valley etc.), the advance of the glacier during the LIA, and the frequency and size of jökulhlaups from glacier dammed lakes. From these descriptions it is known that the glacier terminus advanced at least 5–7 km during the LIA (Jónsson, 2004).

The historical documents describe that the glacier advanced over a vegetated plain (located at ~40–80 m a.s.l.), where now there is an 11 km^2 trench excavated by the glacier. Presently, the trench reaches down to ~300 m below sea level under the current eastern branch of the glacier (Fig. 2). The radio-echo sounding measurements show that around 1.6 km^3 of sediments were eroded by the glacier. Much of this sediment erosion took place during the first half of the 20th century, as indicated by the change in the location of the medial moraine that originates from the nunatak Nỳju-Núpar. Early in the 20th century the moraine was located in the centre of the glacier all the way to the terminus indicating that the terminus area of the glacier was equally fed by the eastern and western branches. The eastern branch currently does not reach the terminus, but stops ~1 km upstream from the present glacier terminus. The present terminus is fed only by the larger western branch. Longitudinal and cross sections in

TCD
5, 1055–1088, 2011

Modelling the 20th and 21st century evolution of Hoffellsjökull glacier

G. Aðalgeirsdóttir et al.

Fig. 3 show the thickness and shape of the glacier at the different times. The maximum thickness of the glacier of ∼560 m is reached about 5 km upstream from the terminus.

A widespread break-up of the over-deepened eastern branch of the terminus area happened in 2010 as is shown in the high resolution Lidar DEM in Fig. 4. This is likely to be the beginning of a formation of a terminus lake with a calving glacier front.

3.2 Mass- and energy balance

The surface mass balance was measured during 1936–1938 by the Swedish–Icelandic expedition, and since the glaciological year 2000/2001, at two locations on the glacier (one close to the terminus and the other in the central part of the accumulation zone), and at two locations close to the western and northern margins of the accumulation zone (Table 1; Fig. 1c). In spring (April–May) cores are drilled through the winter snow layer and the density is measured. Stakes or wires are left in the core holes (in the ablation zone, ∼10 m long wires are drilled into the ice with a steam drill). The summer balance is measured from the extension of the stakes or wires in the spring and late autumn (September–October; Björnsson et al., 1998, 2003). The mass balance and climate conditions during the 1936–1938 Swedish–Icelandic expedition were similar to the first decade of the 21st century (Table 1; Fig. 5).

The mass balance measurements have been supplemented by glacio-meteorological observations at both mass balance sites on the glacier; station Hof at 1200 m a.s.l., slightly above the current ELA, and station HoSpo at 100 m a.s.l. within the ablation zone (Fig. 1). The weather parameters observed on the glacier have been used to calculate the full energy balance at the two AWSs with the methodology described by Guðmundsson et al. (2009a). Both the mass balance and the energy balance data have been used to calibrate and evaluate the PDD mass balance model applied here (see Sect. 5).

3.3 Surface velocity

Horizontal ice velocity has been observed with DGPS equipment at all the mass balance sites (summer and winter velocities based on measurements in spring and again in autumn) and both late summer and annual velocity maps have been deduced from correlation of 2.5 m resolution SPOT5 HRG images (Fig. 6 and Table 2); with an accuracy of about half the pixel size (Berthier et al., 2005). A good spatial coverage was obtained by using two SPOT images from late summer 2002, but reliable signals were only obtained for limited areas when an attempt was made to determine the annual velocity fields from the two late summer SPOT5 images from 2002 and 2003. The ice surface velocity was measured during the 1936–1938 Swedish–Icelandic expedition at several sites along the profile CC' shown in Fig. 3 (Thorarinsson, 1943). The velocities obtained from these measurements are similar to those determined at the same locations from the SPOT5 velocity maps.

3.4 Temperature and precipitation records from meteorological stations

In the present study, the mass balance of Hoffellsjökull is calculated by a model that uses temperature at Hólar in Hornafjörður and precipitation at Fagurhólsmỳri as input parameters (the location of the stations is shown in Fig. 1). Historical temperature and precipitation records from a number of stations around Iceland are available (Figure 1: at Reykjavík since 1871, Fagurhólsmỳri since 1898, Hæll since 1880, Stykkishólmur since 1830, Teigarhorn since 1873, Vestmannaeyjar since 1877, Akureyri in 1846–1854 and after 1881 and Hólar in Hornafjörður in 1884–1890 and after 1921). The temperature records from these stations were used to construct a continuous temperature record for Hólar in Hornafjörður extending back to 1830 using an iterative expectation-maximization (EM) algorithm (Dempster et al., 1977). The precipitation at Fagurhólsmỳri for the period 1857–1924 was estimated using linear regression between the monthly values (separate regression for each month) of temperature at Hólar in Hornafjörður and precipitation at Fagurhólsmỳri, tuned with available precipitation observations (Fig. 5).

TCD
5, 1055–1088, 2011

4 Future climate scenarios

The CES climate scenarios for glacier modelling in Iceland are based on dynamical downscaling of global AOGCM climate change simulations using the A1B emission scenario performed with three RCMs (ECHAM5-r3/DMI-HIRHAM5, HadCM3/MetNo-HIRHAM and ECHAM5-r3/SMHI-RCAO) and a data set of 10 global AOGCM simulations, also based on the A1B emission scenario, submitted by various institutions to the IPCC for its fourth assessment report (IPCC, 2007). These 10 GCMs were chosen from a larger IPCC data set of 22 GCMs based on their surface air temperature (SAT) performance compared with the ERA-40 reanalysis in the period 1958–1998 in an area in the N-Atlantic encompassing Iceland and the surrounding ocean (Nawri and Björnsson, 2010). Based on the downscaled RCM model output the temperature change of the GCM-based scenarios was increased by 25% in the interior of Iceland, where the large ice caps are located, (Nawri and Björnsson, 2010).

Before year 2010, the glacier model is forced with records of observed temperature and precipitation. Possible natural variations in the climate are important for near future projections as the magnitude of the expected anthropogenic change has then not exceeded the random variability of the climate. Therefore, many different climate scenarios were derived for the CES project (Jóhannesson et al., 2011). Expected values of temperature and precipitation in 2010 were estimated by statistical autoregressive (AR) modelling of the past records, thereby taking into account the warming that has been observed in recent years as well as the inertia of the climate system so that the very high temperatures of the last few years have only a moderate effect on the derived expected values. These expected values are intended to represent the deterministic part of the recent variation in the climate when short-term climate variations have been removed by the statistical analysis. Scenarios of the monthly mean temperature and precipitation were calculated from year 2010 to the end of the climate simulation by fitting a least squares line to monthly values simulated by the RCM or GCM from 2010 onwards and shifting the simulated time-series vertically so that the 2010 value of the

TCD
5, 1055–1088, 2011

least squares line matched the expected 2010 value based on the AR modelling of the past climate.

The trend analysis of the future climate eliminates the direct use of a past baseline period in the derivation of the scenarios and provides a consistent match with the recent climate development. Furthermore, the statistical matching of the past climate observations with the trend lines of the future climate provides an implicit bias correction (Jóhannesson et al., 2011). Figure 7 shows the 13 scenarios for annual mean temperature at Hólar in Hornafjörður and precipitation at Fagurhólsmỳri used in this study, compared with the average 2000–2009 climate. The applied scenarios indicate a warming of close to 2.0–2.4°C near the middle of the 21st century with respect to the period 1981–2000, when most of the Icelandic ice caps were close to balance (Guðmundsson et al., 2011; Aðalgeirsdóttir et al., 2006; Guðmundsson et al., 2009b), and by ~3–4°C at the end of the century. With respect to the more recent warmer period 2000–2009, the warming is 1.1–1.5°C near the middle of the 21st century and ~2–3°C by the end of the century. All the scenarios indicate a slight increase in the precipitation during this century (~10%).

5 Models

5.1 Mass balance model

The mass-balance of Hoffellsjökull is simulated with a positive degree-day model (PDD), that has been applied on several Icelandic glaciers, both independently (Jóhannesson et al., 1995, 1997, 2006) and coupled with an ice flow model for Langjökull, Hofsjökull and S-Vatnajökull ice caps (Aðalgeirsdóttir et al., 2006; Guðmundsson et al., 2009b; see locations of the ice caps in Fig. 1). A constant temperature lapse rate, separate degree-day scaling factors for snow (ddf_s) and ice (ddf_i) and linear horizontal and vertical precipitation gradients are used assuming a constant snow/rain threshold of 1 °C. The parameters of the model have been calibrated with available mass balance

TCD
5, 1055–1088, 2011

observations from S-Vatnajökull (up to 23 stakes, Fig. 1) from the mass balance years 1991/1992 to 2004/2005, using temperature at Hólar in Hornafjörður and precipitation at Fagurhólsmỳri as an input. With a temperature gradient of 0.56 °C per 100 m and the degree-day factors $ddf_s = 4.45\,mm_{w.e.}/°C/d$ and $ddf_i = 5.30\,mm_{w.e.}/°C/d$, the model explains 92% and 95% of the annual variations in the winter and summer balance at S-Vatnajökull, respectively (Jóhannesson et al., 2007).

Our model studies show that spatial precipitation variations on Hoffellsjökull are consistent with the linear horizontal and vertical gradients derived for the whole of S-Vatnajökull. This indicates that the mountains surrounding Hoffellsjökull do not generate significant local precipitation patterns. In this study, the temperature gradient and the degree-day factors were further validated for Hoffellsjökull using (i) mass balance stakes on the outlet (three stakes since 2001) and (ii) daily energy balance calculated at the two AWSs on the glacier (Fig. 1). This resulted in the same temperature gradient, and $ddf_s = 4.0 \pm 0.5\ mm_{w.e.}/°C/d$ and $ddf_i = 5.3 \pm 0.7\,mm_{w.e.}/°C/d$ (errors are one standard deviation (σ) of degree-day factors optimized separately for each year).

6 Ice flow model

The dynamic ice flow model is similar as that used by Aðalgeirsdóttir et al., (2006) for Hofsjökull and S-Vatnajökull and Guðmundsson et al., (2009b) for Hofsjökull and Langjökull, except that the numerical implementation in the model applied here uses a staggered finite element method on a triangulated grid rather than a finite difference method to solve the continuity equation (Sigurðsson, 1992), allowing for variable grid size. This model is based on the vertically integrated continuity equation and the shallow ice approximation (SIA), neglecting longitudinal stress gradients and surge dynamics and excludes bed isostatic adjustments and seasonal variations in sliding (Aðalgeirsdóttir, 2003; Aðalgeirsdóttir et al., 2005). The geometry of Hoffellsjökull with a mean thickness of approximately 300 m and length of 20 km (Fig. 3) justifies the application of an ice flow model based on the SIA. Although longitudinal stress gradients and other dynamical complications, ignored by SIA-based models, affect the flow of glaciers in areas of complicated bed geometry, a comparative study has shown that ice volume variations and the retreat and advance rates of a SIA-based model are approximately the same as those computed with a full system model (Leysinger-Vieli and Guðmundsson, 2004). It is therefore appropriate to use a SIA model here for the purpose of studying ice volume variations, large-scale geometry changes and the advance and retreat of Hoffellsjökull.

Basal sliding was not explicitly included in the model used by Aðalgeirsdóttir et al. (2006) and Guðmundsson et al. (2009b), but implicitly included in the calibration of the power-law constitutive relationship (Glen's flow law, Paterson, 1994), which relates strain rate to deviatoric stresses. Aðalgeirsdóttir et al. (2006) and Guðmundsson et al. (2009b) used a series of model runs with a range of the flow parameters to select the parameterization that best simulates the measured glacier geometry. The rate factor (A) calibrated in this manner is on the order of $6.8\times10^{-15}\ \mathrm{s}^{-1}\ \mathrm{kPa}^{-3}$; a value recommended for temperate ice (Paterson, 1994). Here, two approaches are tested: (i) using the same flow law parameter, A, as in the two aforementioned studies, implicitly including basal sliding, and (ii) include a Weertman type sliding law (Paterson, 1994) where the sliding velocity is assumed to be proportional to a power of the basal shear stress, τ_b, ($V_{\mathrm{Slid}} = C \cdot \tau_b^m$); C is the sliding parameter and the exponent $m = 3$ in our calculations. Assuming explicit basal sliding in the model leads to a flow parameter that characterizes stiffer ice (Aðalgeirsdóttir, 2003; Jarosch and Guðmundsson, 2007). A series of model runs were carried out to obtain the flow and sliding parameters for Hoffellsjökull that best simulate the observed evolution of the glacier geometry.

The ice divide is kept at a fixed location in the model computations presented here and no flow is allowed across that boundary. This is not an entirely realistic boundary condition as one may expect the ice divides of the different outlets of the Vatnajökull ice cap to be shifted as a consequence of the response of the ice cap to mass balance variations. As a first approximation, an assumption of fixed boundaries of the main ice flow basins may be assumed to be reasonable because the location of the ice divides is to a large degree controlled by the basal topography. However, this assumption may be expected to become increasingly inaccurate when simulated changes in the geometry of the glacier become relatively large compared with the original size of the glacier.

7 Results

7.1 Steady state experiments

First, steady state experiments (model runs with constant input parameters) were carried out to (i) test the performance of the model, (ii) investigate the stability of the ice geometry (applying directly the observed ice surface geometry as initial state may yield unrealistic transient ice geometry changes due to the model approximations and deficiencies) and (iii) derive an appropriate initial LIA_{max} geometry used to quantify the sensitivity of Hoffellsjökull to changes in individual climatic as well as physical parameters. The year 1895 was chosen as the starting year of the model simulations, as it marks the beginning of warming after the coldest part of the LIA (see temperature time-series in Fig. 5).

The ~1895 LIA_{max} volume of Hoffellsjökull was simulated by running a spin-up of the coupled mass balance – ice flow model (Table 3) assuming the average climate of the coldest recorded period in Iceland from 1860–1890 to remain constant (baseline period 1 in Fig. 5). The average temperature at Hólar in Hornafjörður and precipitation at Fagurhólsmỳri was estimated to be ~1.0°C and ~0.37 $m_{w.e.}$/a, respectively, lower during the period 1860–1890 than in 1981–2000 (baseline period 2 in Fig. 5, Table 4) when most Icelandic ice caps were close to balance, as mentioned earlier. The model was then forced from the simulated LIA_{max} configuration with a step change in temperature and precipitation corresponding to the difference between the periods 1860–1890 and 1981–2000 towards a new steady state. The steady state volume corresponding to the period 1981–2000 was found to be ~10% smaller than the observed volume at that time (Table 3 and the red line in Fig. 8a). Thus, a somewhat colder climate than in 1981–2000 is needed to maintain the size of the glacier it had then.

The three steady state runs shown in Fig. 8a show that the glacier responds to both temperature and precipitation variations. Assuming a warming of $\Delta T=1^{\circ}C$ and no precipitation change ($\Delta P=0\,m_{w.e.}/a$) when going from baseline period 1 to 2 results in a 25% smaller ice volume compared with a simulation when precipitation is also increased (red and green lines in Fig. 8a). This accords with that the frequent low pressure cyclonic systems arriving at the southeast coast of Iceland carrying large amount of precipitation are important for maintaining the glacier.

Figure 8b shows the results of simulations with and without basal sliding indicating that a simulation with ice flow rheology implicitly taking basal sliding into account (red line) in the adopted value of the flow law parameter A (see above) leads to a similar result as a model with explicit basal sliding (green line). This is to be expected as the functional form of the dependency of ice flux on basal sliding through the basal shear stress and ice thickness is very similar to the functional form of the dependency of ice flux on internal deformation (see Paterson, 1994).

Figure 8c shows the sensitivity of the steady state ice volume to the adopted values of the degree-day coefficients for snow and ice, ddf_s and ddf_i. The figure shows that a change in ddf_s has a greater effect than a change in ddf_i of a similar magnitude.

7.2 Reconstruction of the 20th century evolution

The observed 1890 glacier geometry was used as an initial configuration for a simulation through the 20th century, forcing the coupled mass balance – ice flow model with the temperature and precipitation records shown in Fig. 5. The 23% volume reduction of the ice cap from 1895 to 2010 was successfully simulated by the coupled model (Fig. 9a) and the model simulates well the measured volume changes during the 20th century (Table 3). Both ice-flow model approaches were used; with a soft flow parameter, implicitly taking basal sliding into account and including a Weertman type sliding and specifying stiffer ice. Only small differences are found in the volume evolution given by the two methods and a reasonable agreement is obtained between the observed and modeled surface velocity field in both cases (Figs. 6b and c). The

TCD
5, 1055–1088, 2011

modeled velocity in the year 2002 compares well with the spatial pattern of the SPOT derived summer surface velocity, indicating that the model captures the large-scale flow pattern of the glacier.

The 20th century glacier runoff from the area that was ice-covered at LIA_{max} (225 km^2) was computed from the modeled mass balance and precipitation fields (Fig. 9b). The fastest retreat rates and highest runoff rates were obtained for the warm years between 1925 and 1960, and after 2000 (Figs. 5 and 9b).

7.3 Simulation of future response to an ensemble of climate scenarios

The coupled mass balance – ice flow model, calibrated with past observations, was used to simulate the future response of the glacier during the 21st century, using the temperature and precipitation scenarios shown in Fig. 7. For comparison, a model simulation with constant climate corresponding to the last decade was also carried out (~2°C and ~1°C warmer than during the baseline periods 1 and 2, respectively). According to this model run (red dashed curve in Fig. 9a), the ice volume will be reduced by 30% with respect to the 2010 volume (Table 3) at the end of the 21st century (Fig. 9a). If the climate warms as suggested by most of the climate change scenarios, the glacier will have almost disappeared at the end of the 21st century.

The runoff corresponding to the same model runs is shown in Fig. 9b. The runoff from the LIA_{max} ice-covered area is projected to increase for the next 30–40 years and be similar or slightly larger than the runoff during the warm years between 1925 and 1960 when the ice-covered area was considerably larger. The runoff is simulated to start decreasing after ~2050 as a consequence of the reduction in the ice-covered area and approach a level near the end of this century that is similar to the runoff during cooler periods of the 20th century when the glacier was close to equilibrium.

8 Discussion and conclusion

The volume change of Hoffellsjökull from 2001 can be estimated using two independent methods, (i) integrating the surface mass balance (SMB) in Table 1 and the surface area in Table 3, and (ii) integrating the elevation difference between the DEMs over the glaciated area of Hoffellsjökull (dDEMs). Both methods yield the same volume change of $-0.6\pm0.1\,\mathrm{km}^3$ (SMB) and $-0.6\pm0.2\,\mathrm{km}^3$ (dDEMs) from 2001–2008, and $-1.0\pm0.1\,\mathrm{km}^3$ (SMB) and $-1.0\pm0.2\,\mathrm{km}^3$ (dDEMs) from 2001–2010. These results confirm the small estimated errors of the DEMs of 2001, 2008 and 2010 (see Sect. 3).

The model study indicates that a slightly colder climate than observed is necessary to maintain the volume of Hoffellsjökull during the period 1981–2000 (baseline period 2, Fig. 8a, Table 4). This is consistent with the presence of the subglacial trench, excavated by the glacier that lowered the ice surface in the ablation area resulting in increased melting. This could also indicate that in the 1980s to 1990s Hoffellsjökull was responding to the colder climate in the 1960s to 1980s (Fig. 5).

For a given constant reference climate the same glacier volume can be reconstructed by both using a flow parameter $A=6.8\times10^{-15}\,\mathrm{s}^{-1}\,\mathrm{kPa}^{-3}$, for soft ice, implicitly including the basal sliding, as well as with a stiffer ice flow parameter, $A=4.6\times10^{-15}\,\mathrm{s}^{-1}\,\mathrm{kPa}^{-3}$, together with a Weertman type sliding law with a constant sliding parameter, $C=10\times10^{-15}\,\mathrm{m\,a}^{-1}\,\mathrm{Pa}^{-3}$ (Fig. 8b). The same is true for a simulation of the time evolution from 1895 to 2010 (blue and red solid curves in Fig. 9a; Table 3). Using the flow parameter corresponding to stiff ice without adding the sliding leads to a steady state with about ~10% larger ice volume (Fig. 8b). More information about the viscosity of the glacier ice and basal conditions is needed to better distinguish between the contributions of basal sliding and internal deformation to the observed surface velocity (Fig. 6; Table 2).

Model studies of the recovery of depressions formed in the surface of Vatnajökull during a subglacial eruption and subsequent outburst flood in 1996 have been carried out to infer the possible range of the flow parameter, A (Aðalgeirsdóttir et al., 2003, Jarosch and Guðmundsson, 2007). The results indicate that a lower value of A than

TCD
5, 1055–1088, 2011

Modelling the 20th and 21st century evolution of Hoffellsjökull glacier

G. Aðalgeirsdóttir et al.

recommended by Paterson (1994) for temperate ice fits the measurements better. Information about the relative importance of basal sliding may be inferred from seasonal variations in the ice surface velocity. The SPOT velocity maps show 30–50% faster flow within the ablation zone during late summer than the annual average (Fig. 6, Table 2). This indicates a velocity increase due to increased melt water production and/or enhanced basal water pressure during the summer 2002. More data on seasonal velocity variations and on the spatial distribution of the basal sliding are needed to better constrain the model. From the steady state and time evolution model simulations shown in Figs. 8b and 9a and a comparison of the modeled velocity with available surface velocity fields, it is concluded that $A = 4.6 \times 10^{-15}\ \mathrm{s}^{-1}\ \mathrm{kPa}^{-3}$, together with an increased basal sliding during summer, is more realistic than the value $A = 6.8 \times 10^{-15}\ \mathrm{s}^{-1}\ \mathrm{kPa}^{-3}$ recommended by Paterson (1994).

The sensitivity of the model results to the applied degree-day factors was tested by varying the values in the steady state experiments (Fig. 8c). The degree-day factors determined by using mass balance data from the two stakes on Hoffellsjökull and data from the two Automatic Weather Stations are similar to the degree-day factors determined by optimization of 23 mass balance stakes on S-Vatnajökull. The sensitivity tests show that varying the degree-day factors by the standard deviation obtained from an optimization for each year separately does not have a major impact on the steady state volume (Fig. 8c). It is therefore concluded that the degree-day parameters, optimized by the available mass and energy balance data, are appropriate for the coupled surface mass balance – ice flow model.

Runoff from the area covered by the LIA_{max} glacier for the whole modeled period 1895–2100 is shown in Fig. 9b. The runoff includes both precipitation and snow and ice melt. The results show large interannual variability as well as an increase in runoff with temperature. It should be noted that this model output cannot be validated against observations as no river discharge measurements are available from this area and mass balance is only measured at two stakes on the glacier. Towards the end of the simulation the runoff is reduced because the glacier has nearly disappeared. Even

TCD
5, 1055–1088, 2011

though there is a large spread depending on the applied scenario, the general trend of an initial increase, followed by a decrease in runoff during the second half of the 21st century is similar for most of the scenarios. It is found that until ∼2030, apparently random natural climate variations lead to interannual runoff variations of a similar magnitude as the average runoff increase with respect to the period 1981–2000. Around the middle of the century, most of the climate change scenarios indicate that the deterministic part of the simulated runoff change due to the warming of the long-term climate has become larger than the magnitude of the interannual variations.

Acknowledgements. We acknowledge the support for this project from the Icelandic Research Fund (Rannís), the University Research Fund, the support of the Public Roads Administration, the National Power Company of Iceland, the Nordic Project Climate and Energy Systems (CES) supported by Nordic Energy Research, Alþingi (Parliament of Iceland) and the "Jules Verne" French–Icelandic program. SPOT 5 HRG images were made available by the French Space Agency (CNES) through the ISIS (Incentive for the Scientific use of Images from the SPOT system) program and SPOT 5 HRS digital elevation models by the Spot Image project Planet Action (www.planet-action.org) and the SPIRIT (SPOT 5 stereoscopic survey of Polar Ice: Reference Images and Topographies) international Polar Year (IPY) project. E.B. acknowledges support by the TOSCA (CNES) and PNTS programs. The 2010 Lidar digital elevation map was acquired as a part of an ongoing effort to map the surface of Icelandic ice caps, started in the International Polar Year 2007–2009. We thank Egill Jónsson for enthusiastic support, Sveinbjörn Steinþórsson, Kirsty Ann Langley, Þorsteinn Jónsson, Hannes H. Haraldsson and Gunnar Páll Eydal for extensive field work, Gísli Sigurbergsson the farmer at Svínafell for his voluntary participation in field work and other assistance and Eyjólfur Magnússon for constructive discussion on error analysis.

References

Aðalgeirsdóttir, G.: Flow dynamics of Vatnajökull ice cap, Iceland, Mitteilung 181, Versuchsantalt fur Wasserbau, Hydrologie und Glaziologie der ETH Zurich-Zentrum, 178 pp, 2003.

Aðalgeirsdóttir, G., Jóhannesson, T., Björnsson, H., Pálsson, F., Sigurðsson, O.: Response of Hofsjökull and southern Vatnajökull, Iceland, to climate change, J. Geophys. Res.,111, F03001, doi:10.1029/2005JF000388, 2006.

Aðalgeirsdóttir, G., Björnsson, H., and Jóhannesson, T.: Vatnajökull ice cap, results of computations with a dynamical model coupled with a degree-day mass-balance model, Reykjavík, Science Institute, University of Iceland, Rep. RH-11-2004, 2004.

Ahlmann, H. W.: The regime of Hoffellsjökull, Geografiska Annaler, 21, 171–188, 1939.

Ahlmann, H. W. and Thorarinsson, S.: Vatnajökull, Scientific results of the Swedish–Icelandic investigations 1936–37–38, Stockholm, Esselte, 306 pp, 1943.

Berthier, E., Vadon, H., Baratoux, D., Arnaud, Y., Vincent, C., Feigl, K. L., Rémy, F. and Legrésy, B.: Surface motion of mountain glaciers derived from satellite optical imagery, Remote Sens. Environ., 95(1), 14–28, 2005.

Björnsson, H.: The surface area of glaciers in Iceland, Jökull, 28, 31, 1978.

Björnsson, H.: Glaciers in Iceland, Jökull, 29, 74–80, 1979.

Björnsson, H., Pálsson, F., and Haraldsson, H. H.: Mass balance of Vatnajökull (1991–2001) and Langjökull (1996–2001), Iceland, Jökull, 53, 75–78, 2003.

Björnsson, H. and Pálsson, F.: Jöklar í Hornafirði, in: Björnsson, H., Jónsson, E., and Runólfsson, S., Jöklaveröld, Náttúra og Mannlíf, Reykjavík, Skrudda, 125–164, 2004.

Björnsson, H. and Pálsson, F.: Icelandic glaciers. Jökull, 58, 365–386, 2008.

Bouillon, A., Bernard, M., Gigord, P., Orsoni, A., Rudowski, V., and Baudoin, A.: SPOT 5 HRS geometry performance: Using block adjustments as a key issue to improve quality of DEM generation, ISPRS Journal of Photogrammetry and Remote Sensing, 60, 134–146, 2006.

Dempster, A. P., Laird, N. M., and Rubin, D. B.: Maximum likelihood from incomplete data via the EM algorithm, J. Roy. Statist. Soc., Ser. B, 39(1), 1–38, 1977.

Einarsson, M. Á.: Climate of Iceland, edited by: van Loon, H., Climates of the Oceans, Elsevier, Amsterdam, 673–697, 1984.

Guðmundsson, S., Björnsson, H., Pálsson, F., and Haraldsson, H. H.: Energy balance and degree-day models of summer ablation on the Langjökull ice cap, SW Iceland, Jökull, 59, 1–18, 2009a.

Guðmundsson, S., Björnsson, H., Jóhannesson, T., Aðalgeirsdóttir, G., Pálsson, F., and Sigurðsson, O.: Similarities and differences in the response of two ice caps in Iceland to climate warming, Hydrol. Res., 40, 495–502, 2009b.

Guðmundsson, S., Björnsson, H., Magnússon, E., Berthier, E., Pálsson, F., Guðmundsson, M. T., Högnadóttir, Th., and Dall, J.: Response of Eyjafjallajökull, Torfajökull and Tindfjallajökull

ice caps in Iceland to regional warming, deduced by remote sensing, Polar Res., in press., 2011.
IPCC: Climate Change 2007: The Physical Science Basis, Contribution of Working Group I to the Fourth Assessment Report of the Intergovernmental Panel on Climate Change, edited by: Solomon, S., Qin, D., Manning, M., Chen, Z., Marquis, M., Averyt, K. B., Tignor, M., and Miller, Jr, H. L., Cambridge, UK, and New York, NY, USA, Cambridge University Press, 996 pp., 2007.
Jarosch, A. H. and Guðmundsson, M. T.: Numerical studies of ice flow over subglacial geothermal heat sources at Grímsvötn, Iceland, using Full Stokes equations, J. Geophys. Res.-Earth, 112, F02008, doi:10.1029/2006JF000540, 2007.
Jóhannesson, T., Sigurðsson, O., Laumann, T., and Kennett, M.: Degree-day glacier mass-balance modelling with application to glacier in Iceland, Norway and Greenland, J. Glaciol., 41(138), 345–358, 1995.
Jóhannesson, T.: The response of two Icelandic glaciers to climatic warming computed with a degree-day glacier mass balance model coupled to a dynamic glacier model, J. Glaciol., 43(143), 321–327, 1997.
Jóhannesson, T., Sigurðsson, O., Einarsson, B., and Thorsteinsson, Th.: Mass-balance modelling of the Hofsjökull ice cap based on data from 1988–2004, Reykjavík, National Energy Authority, Rep. OS-2006/004, 2006.
Jóhannesson, T., Aðalgeirsdóttir, G., Björnsson, H., Crochet, P., Elíasson, E. B., Guðmundsson, S., Jónsdóttir, J. F., Ólafsson, H., Pálsson, F., Rögnvaldsson, Ó., Sigurðsson, O., Snorrason, Á., Blöndal Sveinsson, Ó. G., and Thorsteinsson, Th.: Effect of climate change on hydrology and hydro-resources in Iceland. Reykjavík, National Energy Authority, Rep. OS-2007/011, 2007.
Jóhannesson, T., Aðalgeirsdóttir, G., Ahlstrøm, A., Andreassen, L. M., Beldring, S., Björnsson, H., Crochet, P., Einarsson, B., Elvehøy, H., Guðmundsson, S., Hock, R., Machguth, H., Melvold, K., Pálsson, F., Radić, V., Sigurðsson, O., and Thorsteinsson, Th.: Hydropower, snow and ice, edited by: Thorsteinsson, Th. and Björnsson, H., Climate Change and Energy Systems, Impacts, Risks and Adaptation in the Nordic Countries, Copenhagen, Nordic Council of Ministers, Nord, 2011.
Jónsson, E.: Í veröld jökla, sanda og vatna, edited by: Björnsson, H., Jónsson, E., and Runólfsson, S., Jöklaveröld, Náttúra og Mannlíf, Reykjavík, Skrudda, 11–86, 2004.
Korona, J., Berthier, E., Bernard, M., Remy, F., and Thouvenot, E.: SPIRIT. SPOT 5 stereo-

scopic survey of Polar Ice: Reference images and topographies during the fourth International Polar Year (2007–2009), ISPRS Journal of Photogrammetry and Remote Sensing, 64, 204–212, 2009.
Leysinger Vieli, G. J.-M. C. and Guðmundsson, G. H.: On estimating length fluctuations of glaciers caused by changes in climatic forcing, J. Geophys. Res., 109, F01007, doi:10.1029/2003JF000027, 2004.
Nawri, N. and Björnsson, H.: Surface air temperature and precipitation trends for Iceland in the 21st century, Reykjavík, Icelandic Meteorological Office, Rep. 2010–005, 2010.
Paterson, W. S. B.: The Physics of Glaciers, 3 Edn., Elsevier, Oxford, 1994.
Sigurðsson, S.: Treatment of the Convective Term in Staggered Finite Element Schemes for Shallow Water Flow, edited by: Russel, T. F., Brebbia, C. A., Gray, W. G., and Pinder, G. F., Computational Methods in Water Resources IX, Vol. 1: Numerical Methods in Water Resources. ComputationalMechanics Publications, Elsevier Applied Science, 291–98, 1992.
Sigurðsson, O. and Jóhannesson: Interpretation of glacier variations in Iceland 1930–1995, Jökull, 45, 27–33, 1995.
Thorarinsson, S.: Hoffellsjökull, its movement and drainage. Geografiska Annaler, 21, 189–215, 1939.
Thorarinsson, S.: Vatnajökull. Scientific results of the Swedish–Icelandic investigations 1936–37–38, Ch. XI: Oscillations of the Iceland glaciers in the last 250 years, Geografiska Annaler, 25, 1–54, 1943.

TCD
5, 1055–1088, 2011

Modelling the 20th and 21st century evolution of Hoffellsjökull glacier

G. Aðalgeirsdóttir et al.

Table 1. Winter (b_w), summer (b_s) and net balance (b_n) for Hoffellsjökull in $m_{w.e.}\ a^{-1}$. A conservative error estimate is on the order of 10%.

Glacier year	b_w	b_s	b_n
1935–1936	2.0	−3.4	−1.4
1936–1937	2.4	−2.1	0.3
1937–1938	1.7	−2.4	−0.6
2000–2001	1.3	−2.1	−0.8
2001–2002	2.3	−1.8	0.5
2004–2005	1.1	−2.7	−1.6
2005–2006	1.9	−2.6	−0.7
2006–2007	1.8	−2.3	−0.5
2007–2008	1.9	−2.6	−0.7
2008–2009	2.1	−2.4	−0.3
2009–2010	1.8	−3.4	−1.6

TCD
5, 1055–1088, 2011

Table 2. Average annual (September 2002 to September 2003; accuracy ~2 m a^{-1}) and late summer (27 August and 22 September 2002; accuracy ~20 m a^{-1}) velocities deduced from cross-correlation of 2.5 m resolution SPOT5 HRG satellite images. Coherence of the annual velocity signal was only obtained in the vicinity of the locations 1–3 shown in Fig. 6a.

Location	1	2	3
Annual velocity (m a^{-1})	360	110	120
Late summer velocity (m a^{-1})	550	140	150

TCD
5, 1055–1088, 2011

Table 3. (a–b) Observed volume and area of Hoffellsjökull. (c) Simulated volume using $A = 6.8 \times 10^{-15}\,\mathrm{s^{-1}\,kPa^{-3}}$ implicitly including the basal sliding. (d) Simulated volume using $A = 4.6 \times 10^{-15}\,\mathrm{s^{-1}\,kPa^{-3}}$ and $C = 10 \times 10^{-15}\,\mathrm{m\,a^{-1}\,Pa^{-3}}$. All volumes correspond to autumn; the 2001 spring volume is corrected with the summer balance in Table 1. Displayed errors (random for each year) are calculated using the standard error formula and the uncertainties of the surface maps. In addition, there is an uncertainty of $<3\,\mathrm{km^3}$ (same bias for all years), due to errors in the bedrock map.

Year	~ 1895	1936	1946	1986	2001	2008	2010
(a) Vo ($\mathrm{km^3}$)	69 ± 4	63 ± 3	61 ± 2	58 ± 1	55.2 ± 0.2	54.6 ± 0.1	54.2 ± 0.0
(b) Ao ($\mathrm{km^2}$)	234 ± 4	228 ± 4	224 ± 3	216 ± 2	212 ± 1	209 ± 0.5	206 ± 0.5
(c) Vs ($\mathrm{km^3}$)	68.9	64.5	61.5	55.6	54.8	52.9	52.4
(d) Vs ($\mathrm{km^3}$)	68.9	64.4	61.4	55.4	54.5	52.7	52.2

Table 4. (b–c) Temperature at Hólar in Hornafjörður and precipitation at Fagurhólsmỳri, averaged over the years from t_1 to t_2. (d) Volume at the year t_2; from Table 3. (e) Volume of a stable spin-up glacier corresponding to the average climate over the years t_1–t_2 (initialised with the reconstructed 1895 geometry).

(a) t_1–t_2 (years)	(b) T (°C)	(c) P (m/a)	(d) Vo (km^3)	(e) Vs (km^3)
1860–1890	~ 3.52	~ 1.43	69 ± 4	68.3
1981–2000	4.53	1.80	55.2 ± 0.2	50.6

TCD
5, 1055–1088, 2011

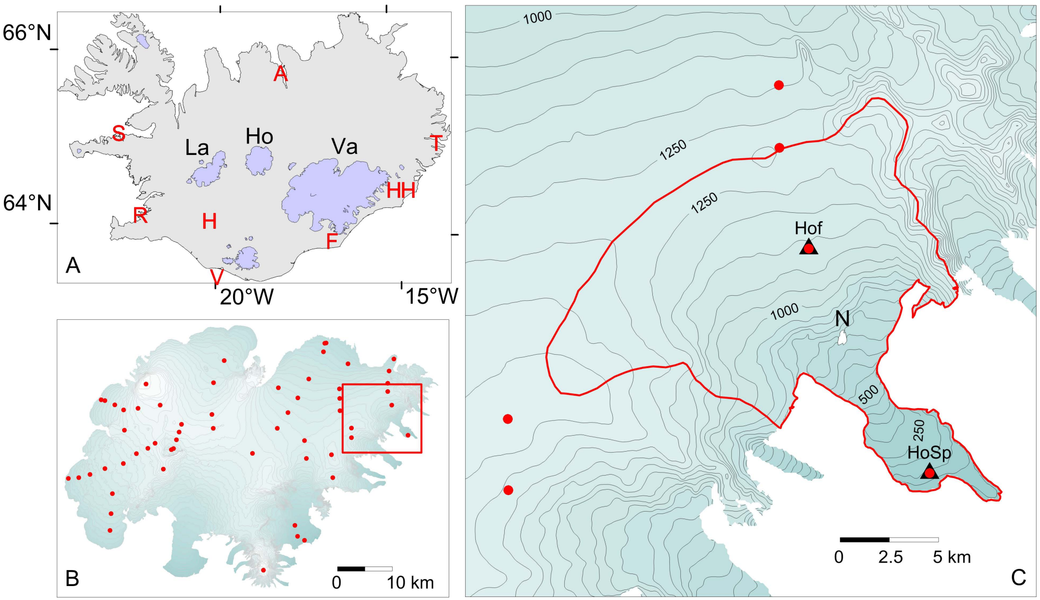

Fig. 1. **(A)** Iceland and the largest ice caps, Vatnajökull (Va), Hofsjökull (Ho) and Langjökull (La). Locations of the weather stations, used to reconstruct the temperature and precipitation records, are shown with letters: Reykjavík (R), Fagurhólmỳri (F), Hæll (H), Stykkishólmur (S), Teigarhorn (T), Vestamannaeyjar (V), Akureyri (A) and Hólar in Hornafjörður (HH). **(B)** The surface topography of Vatnajökull ice cap. Red dots show the sites of mass balance and velocity measurements and the red box the position of the frame to the right. **(C)** Hoffellsjökull. The ice divide and the model domain are indicated with the red curve enclosing a glaciated area of ∼212 km^2 at the year 2001. Black triangles show the locations of automatic weather stations on the glacier. N is the location of the central nunatak Nỳju Núpar.

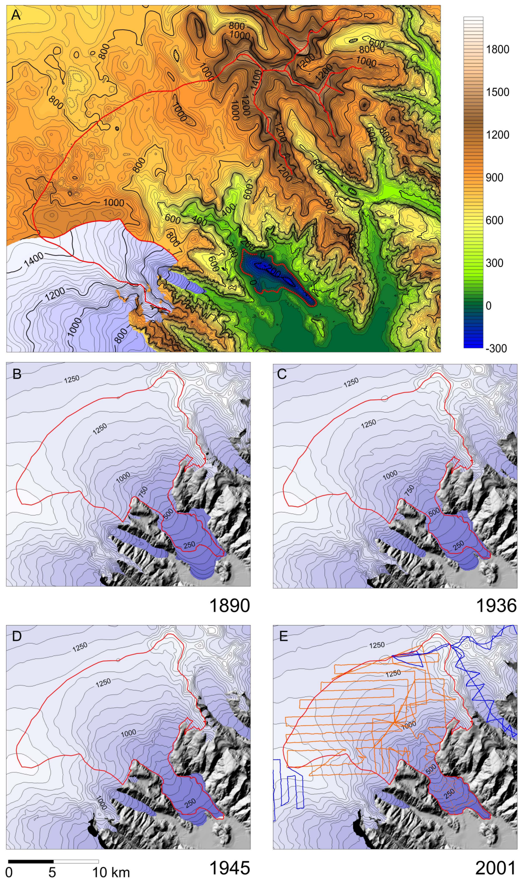

Fig. 2. **(A)** Measured bedrock topography of Hoffellsjökull. Blue colours indicate elevation below sea level. **(B–E)** Surface topography at different times, showing retreat and thinning during the 20th century. The location of the radio-echo sounding lines is shown in **E**). The red line is the 2001 ice divide for Hoffellsjökull (212 km^2).

TCD
5, 1055–1088, 2011

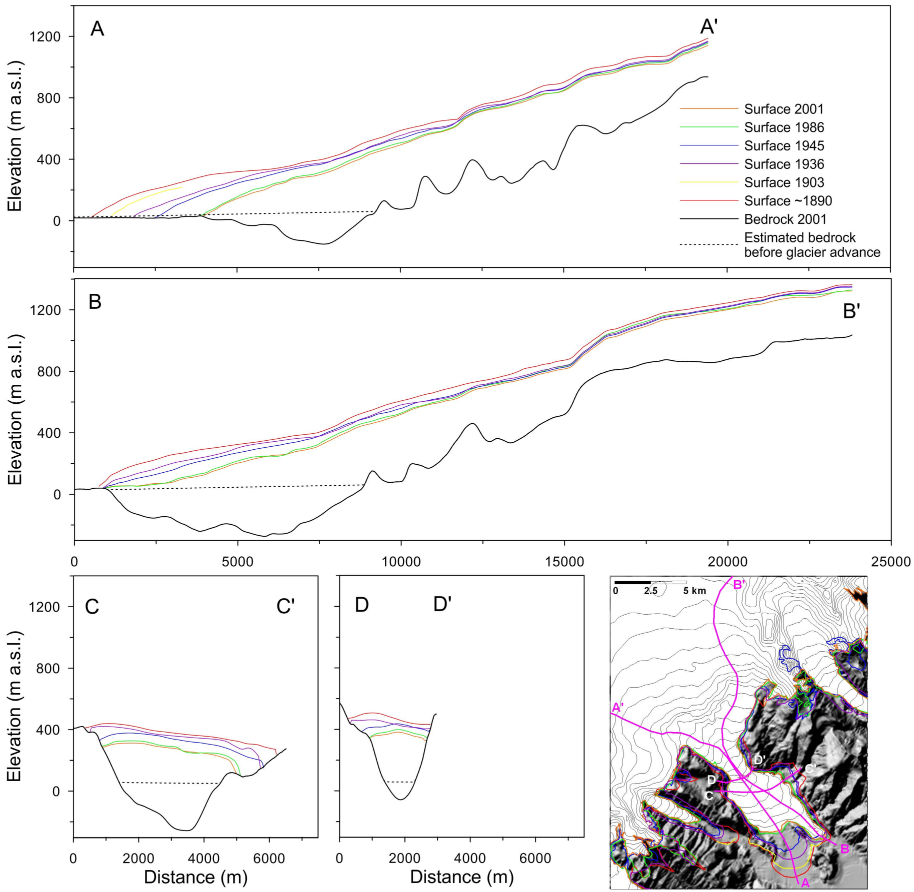

Fig. 3. Two longitudinal profiles and two cross sections showing the thickness and the location of the terminus. The map shows the location of the sections and the terminus position at the different times.

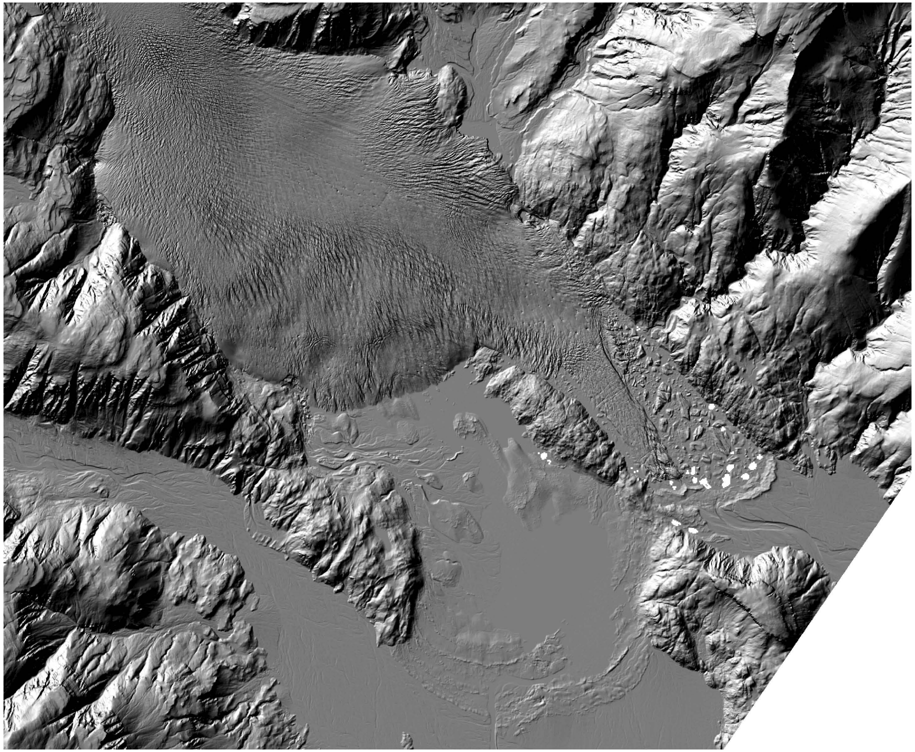

Fig. 4. A topographic relief shading showing the August 2010 Lidar DEM of the terminus and the lower part of Hoffellsjökull. The LIA terminus moraines can be seen in front of the terminus as well as the extensive break-up of the eastern branch of the terminus into the lake in front of the glacier that occurred in 2010.

TCD
5, 1055–1088, 2011

Modelling the 20th and 21st century evolution of Hoffellsjökull glacier

G. Aðalgeirsdóttir et al.

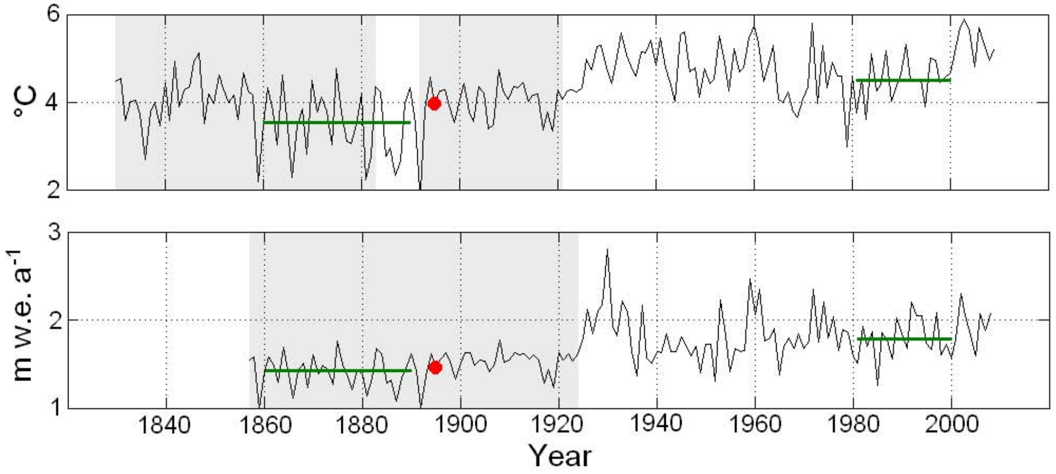

Fig. 5. Temperature (top) at Hólar in Hornafjörður and precipitation (bottom) at Faghurhólsmỳri. The gray areas indicate the periods when the time-series were reconstructed. The horizontal lines indicate the average climate for the two baseline periods 1860–1890 (period 1, used to reconstruct a spin-up LIA$_{max}$ geometry corresponding to the year 1895) and 1981–2000 (period 2, a period when many Icelandic ice caps were close to balance). The dots show the temperature and precipitation in 1895, the first year of the model simulations.

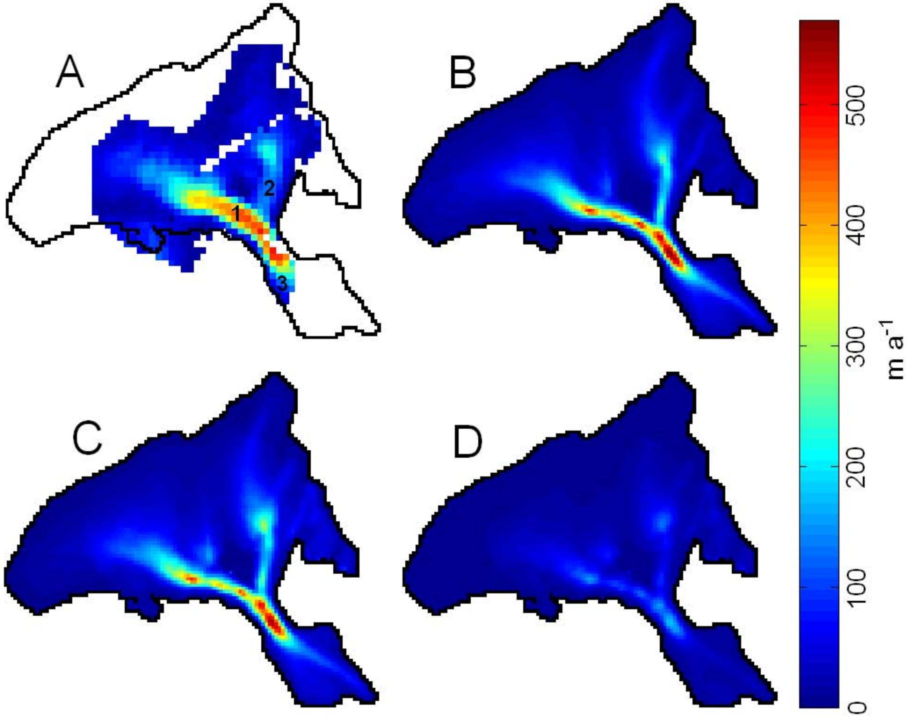

Fig. 6. **(A)** Late summer ice surface velocity determined by cross-correlation of 2.5 m resolution SPOT5 HRG satellite images acquired on 27 August and 22 September 2002. The numbers 1–3 point out locations where annual surface velocity signal could be deduced by correlating two SPOT5 HRG satellite images from late September 2002 and 2003 (see Table 2). **(B–C)** Depth–averaged modeled ice velocity corresponding to the simulated 2002 ice surface geometry, using $A = 6.8 \times 10^{-15}\ \mathrm{s^{-1}\ kPa^{-3}}$ implicitly including the basal sliding (in **B**)), and using $A = 4.6 \times 10^{-15}\ \mathrm{s^{-1}\ kPa^{-3}}$ and $C = 10 \times 10^{-15}\ \mathrm{m\ a^{-1}\ Pa^{-3}}$ (in **C**). **(D)** The contribution of the modeled basal sliding to the velocity shown in **(C)**.

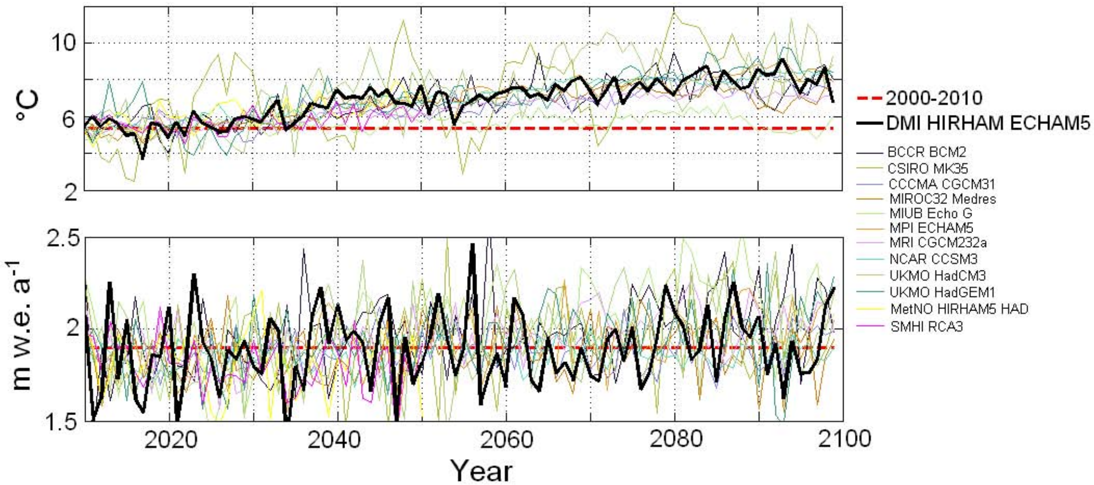

Fig. 7. Temperature at Hólar in Hornafjörður (top) and precipitation at Fagurhólsmỳri (bottom); scenarios from the Nordic CES Project. The average climate of 2000–2009 is plotted for comparison (dashed line). The DMI HIRHAM ECHAM5 climate scenario is highlighted as it is near the middle of the thirteen climate change scenarios.

TCD
5, 1055–1088, 2011

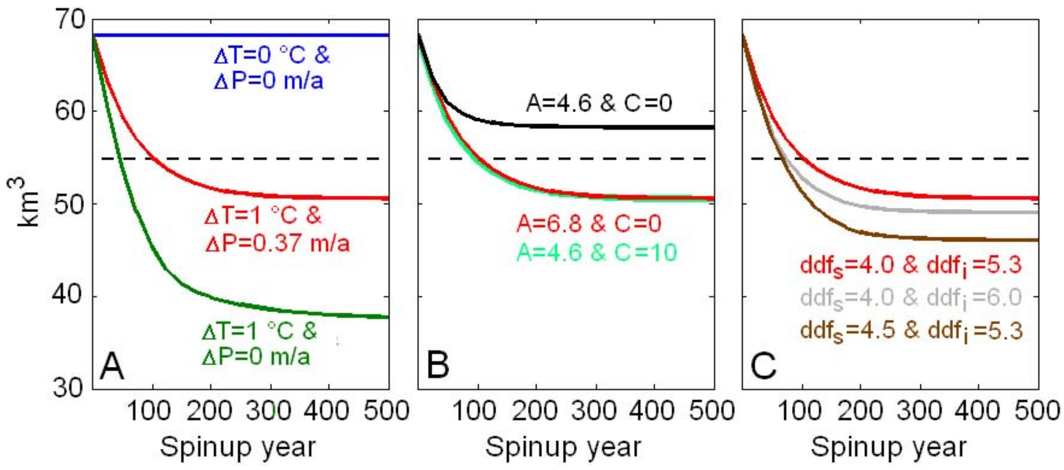

Fig. 8. **(A)** Steady state volume of the model glacier corresponding to the 1860–1890 baseline climate ($\Delta T = 0^{\circ}$C and $\Delta P = 0$ m/a; Table 1 and Fig. 5) and sensitivity of the model to step changes in T and P (the 1981–2000 baseline climate corresponds to $\Delta T = 1^{\circ}$C & $\Delta P = 0.37$ m/a). The dashed straight line shows the 2001 measured volume (55.2 km^3). **(B)** Sensitivity to the rate flow parameter A (in 10^{-15} s^{-1} kPa^{-3}) and the sliding parameter C (in 10^{-15} m a^{-1} Pa^{-3}). **(C)** Sensitivity to shift by one σ of ddf$_s$ and ddf$_i$ (in mm$^{\circ}_{\text{w.e.}}$C^{-1} d^{-1}). In **(A)** and **(B)** $A = 6.8 \times 10^{-15}$ s^{-1} kPa^{-3}, $C = 0$ (no sliding); in **(A)** and **(C)** ddf$_s = 4.0$ mm$^{\circ}_{\text{w.e.}}$C^{-1} d^{-1} and ddf$_i = 5.3$ mm$^{\circ}_{\text{w.e.}}$C^{-1} d^{-1}; in **(B)** and **(C)** the reference climate of 1981–2000 is kept fixed. Note: in all the model runs, the initial ice surface is the steady spin-up state corresponding to 1895 (Table 1) and the red curve is the same in **A, B** and **C** (same model run).

TCD
5, 1055–1088, 2011

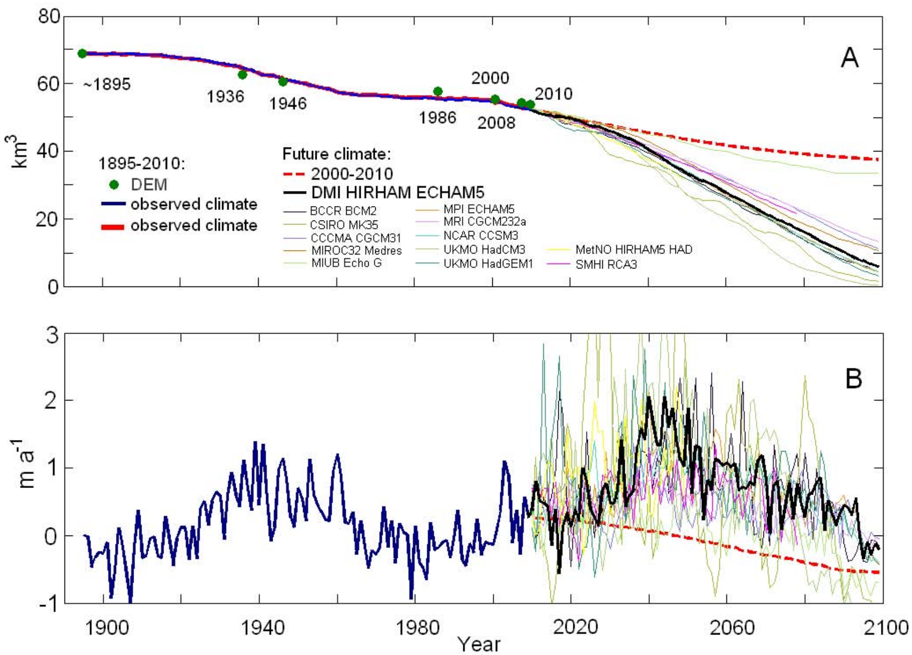

Fig. 9. (A) Simulated evolution of Hoffellsjökull ice volume during the 20th and 21st centuries, initiated with the observed ∼1895 LIA_{max} glacier geometry. The green dots are volume estimates from DEMs. The volume change 1895–2010 is simulated by using the T and P records in Fig. 5 along with (i) $A = 6.8 \times 10^{-15}\ \text{s}^{-1}\ \text{kPa}^{-3}$ implicitly including the basal sliding (blue curve) and (ii) $A = 4.6 \times 10^{-15}\ \text{s}^{-1}\ \text{kPa}^{-3}$ and $C = 10 \times 10^{-15}\ \text{m a}^{-1}\ \text{Pa}^{-3}$ (red curve). The future evolution is computed by using the climate scenarios in Fig. 7 and by maintaining the average climate of 2000–2009 (dashed red curve). **(B)** Simulated specific runoff changes (precipitation and glacier melt) from the area covered by the LIA_{max} glacier (∼234 km^2). Uncertainties of the DEM derived volume numbers are given in Table 3.

TCD

5, 1055–1088, 2011

Modelling the 20th and 21st century evolution of Hoffellsjökull glacier

G. Aðalgeirsdóttir et al.